



THE UNIVERSITY *of* EDINBURGH

Edinburgh Research Explorer

Dynamical behaviour and stability analysis of hydromechanical gates

Citation for published version:

Bernhard, F & Perona, P 2017, 'Dynamical behaviour and stability analysis of hydromechanical gates', *Journal of Irrigation and Drainage Engineering*, vol. 143, no. 9. [https://doi.org/10.1061/\(ASCE\)IR.1943-4774.0001209](https://doi.org/10.1061/(ASCE)IR.1943-4774.0001209)

Digital Object Identifier (DOI):

[10.1061/\(ASCE\)IR.1943-4774.0001209](https://doi.org/10.1061/(ASCE)IR.1943-4774.0001209)

Link:

[Link to publication record in Edinburgh Research Explorer](#)

Document Version:

Peer reviewed version

Published In:

Journal of Irrigation and Drainage Engineering

General rights

Copyright for the publications made accessible via the Edinburgh Research Explorer is retained by the author(s) and / or other copyright owners and it is a condition of accessing these publications that users recognise and abide by the legal requirements associated with these rights.

Take down policy

The University of Edinburgh has made every reasonable effort to ensure that Edinburgh Research Explorer content complies with UK legislation. If you believe that the public display of this file breaches copyright please contact openaccess@ed.ac.uk providing details, and we will remove access to the work immediately and investigate your claim.



Journal of Irrigation and Drainage Engineering

Dynamical Behaviour and Stability Analysis of Hydromechanical Gates

--Manuscript Draft--

Manuscript Number:	IRENG-8017R1	
Full Title:	Dynamical Behaviour and Stability Analysis of Hydromechanical Gates	
Manuscript Region of Origin:	SWITZERLAND	
Article Type:	Technical Paper	
Manuscript Classifications:	91.30000: Hydraulic Structure Design & Management; 91.32000: Control structures; 91.64000: Surface water control systems; 91.64200: Canals; 97: Irrigation & Drainage	
Funding Information:	Schweizerischer Nationalfonds zur Förderung der Wissenschaftlichen Forschung (PP00P2153028/1)	Paolo Perona
Abstract:	<p>This study revisits the stability of hydromechanical gates for upstream water surface regulation, also known as AMIL gates.</p> <p>AMIL gates are used in irrigation canals, where they are often installed in series. From the regulation perspective, instabilities are undesired, as they generate waves and fluctuations in the discharge.</p> <p>We describe a mathematical model for an AMIL gate as a nonlinear dynamical system, which permits to analyse the dynamic interaction between the local water level and the gate position.</p> <p>The feedback effect of the gate on the water level is introduced by considering a storage volume of length l.</p> <p>In the derived model, waves are simplified to fluctuations of the flat water surface of the storage volume.</p> <p>Although previous studies used the same model, none has clarified the sensitivity of the model to the parameter l.</p> <p>The role of this parameter is investigated and it is calibrated with experimental measurements.</p> <p>The precision of the regulation is described by the decrement, the range of the water level around the target level.</p> <p>Based on the mathematical model, a relationship for calibration of the gate and precision of regulation is presented.</p> <p>The subsequent stability analysis of the dynamical system focuses on five control parameters and sheds light on their influence on the gate behaviour.</p> <p>Hopf bifurcations are identified, which separate stable equilibrium solutions from stable periodic solutions.</p> <p>Further work might consider the implications of the periodic solutions on gates that work in series, as well as envision the innovative use of such gates outside of the domain of irrigation canals to obtain dynamic environmental flows in hydropower systems.</p>	
Corresponding Author:	Fabian Bernhard Lausanne, SWITZERLAND	
Corresponding Author E-Mail:	fabian.bernhard@epfl.ch;mail@fber.ch	
Order of Authors:	Fabian Alexander Bernhard Paolo Perona	
Additional Information:		
Question	Response	
Authors are required to attain permission to re-use content, figures, tables, charts, maps, and photographs for which the authors do not hold copyright. Figures	No	

<p>created by the authors but previously published under copyright elsewhere may require permission. For more information see http://ascelibrary.org/doi/abs/10.1061/9780784479018.ch03. All permissions must be uploaded as a permission file in PDF format. Are there any required permissions that have not yet been secured? If yes, please explain in the comment box.</p>	
<p>ASCE does not review manuscripts that are being considered elsewhere to include other ASCE Journals and all conference proceedings. Is the article or parts of it being considered for any other publication? If your answer is yes, please explain in the comments box below.</p>	No
<p>Is this article or parts of it already published in print or online in any language? ASCE does not review content already published (see next questions for conference papers and posted theses/dissertations). If your answer is yes, please explain in the comments box below.</p>	No
<p>Has this paper or parts of it been published as a conference proceeding? A conference proceeding may be reviewed for publication only if it has been significantly revised and contains 50% new content. Any content overlap should be reworded and/or properly referenced. If your answer is yes, please explain in the comments box below and be prepared to provide the conference paper.</p>	No
<p>ASCE allows submissions of papers that are based on theses and dissertations so long as the paper has been modified to fit the journal page limits, format, and tailored for the audience. ASCE will consider such papers even if the thesis or dissertation has been posted online provided that the degree-granting institution requires that the thesis or dissertation be posted.</p> <p>Is this paper a derivative of a thesis or dissertation posted or about to be posted on the Internet? If yes, please provide the URL or DOI permalink in the comment box below.</p>	No
<p>Each submission to ASCE must stand on its own and represent significant new information, which may include disproving</p>	No

<p>the work of others. While it is acceptable to build upon one's own work or replicate other's work, it is not appropriate to fragment the research to maximize the number of manuscripts or to submit papers that represent very small incremental changes. ASCE may use tools such as CrossCheck, Duplicate Submission Checks, and Google Scholar to verify that submissions are novel. Does the manuscript constitute incremental work (i.e. restating raw data, models, or conclusions from a previously published study)?</p>	
<p>Authors are expected to present their papers within the page limitations described in Publishing in ASCE Journals: A Guide for Authors. Technical papers and Case Studies must not exceed 30 double-spaced manuscript pages, including all figures and tables. Technical notes must not exceed 7 double-spaced manuscript pages. Papers that exceed the limits must be justified. Grossly over-length papers may be returned without review. Does this paper exceed the ASCE length limitations? If yes, please provide justification in the comments box below.</p>	<p>Yes</p>
<p>If yes, please provide justification in the comments box below. as follow-up to "Authors are expected to present their papers within the page limitations described in Publishing in ASCE Journals: A Guide for Authors. Technical papers and Case Studies must not exceed 30 double-spaced manuscript pages, including all figures and tables. Technical notes must not exceed 7 double-spaced manuscript pages. Papers that exceed the limits must be justified. Grossly over-length papers may be returned without review. Does this paper exceed the ASCE length limitations? If yes, please provide justification in the comments box below. "</p>	<p>The article text remains below the limit of 10,000 words, however including figures the manuscript is slightly longer than 30 pages.</p> <p>Given the (dynamical systems) approach we use, we think that the number of figures is important to better deliver the message to the audience of this journal, hence the exceeding page number.</p>
<p>All authors listed on the manuscript must have contributed to the study and must approve the current version of the manuscript. Are there any authors on the paper that do not meet these criteria? If the answer is yes, please explain in the comments.</p>	<p>No</p>
<p>Was this paper previously declined or</p>	<p>Yes</p>

<p>withdrawn from this or another ASCE journal? If so, please provide the previous manuscript number and explain what you have changed in this current version in the comments box below. You may upload a separate response to reviewers if your comments are extensive.</p>	
<p>Please provide the previous manuscript number and explain what you have changed in this current version in the comments box below. You may upload a separate response to reviewers if your comments are extensive.</p> <p>as follow-up to "Was this paper previously declined or withdrawn from this or another ASCE journal? If so, please provide the previous manuscript number and explain what you have changed in this current version in the comments box below. You may upload a separate response to reviewers if your comments are extensive."</p>	<p>HYENG-10385</p> <p>We do not understand why the paper was not considered as a case for a technical paper (see Editor's Comments below).</p> <p>We do not want to shorten it to a technical note and decided submitting it here, as, at this point, this journal is more appropriate.</p> <p>"Editor's Comments [HYENG-10385]:</p> <p>The paper does not provide the grounds for considering it as a technical paper. Therefore, the paper has not undergone under peer review. The authors could shorten it to less than 3,000 words and focus on a sensitivity analysis (and submit it as a tech note) or choose to submit somewhere else."</p>
<p>Companion manuscripts are discouraged as all papers published must be able to stand on their own. Justification must be provided to the editor if an author feels as though the work must be presented in two parts and published simultaneously. There is no guarantee that companions will be reviewed by the same reviewers, which complicates the review process, increases the risk for rejection and potentially lengthens the review time. If this is a companion paper, please indicate the part number and provide the title, authors and manuscript number (if available) for the companion papers along with your detailed justification for the editor in the comments box below. If there is no justification provided, or if there is insufficient justification, the papers will be returned without review.</p>	
<p>If this manuscript is intended as part of a Special Issue or Collection, please provide the Special Collection title and name of the guest editor in the comments box below.</p>	
<p>Recognizing that science and engineering are best served when data are made available during the review and discussion of manuscripts and journal articles, and to allow others to replicate and build on work published in ASCE journals, all reasonable requests by reviewers for materials, data, and associated protocols must be fulfilled. If you are restricted from sharing your data and</p>	

materials, please explain below.	
Papers published in ASCE Journals must make a contribution to the core body of knowledge and to the advancement of the field. Authors must consider how their new knowledge and/or innovations add value to the state of the art and/or state of the practice. Please outline the specific contributions of this research in the comments box.	This work deals with a dynamical system approach to model the coupled behaviour between a canal and a hydromechanical gate. We revisit the level pool approach under a more comprehensive framework, which allows to inquire nonlinear issues of the coupled dynamics. This analysis complements existing studies and concludes with useful hints towards the possible use of such gates in operating dynamic environmental flow releases in modern hydropower plants.
The flat fee for including color figures in print is \$800, regardless of the number of color figures. There is no fee for online only color figures. If you decide to not print figures in color, please ensure that the color figures will also make sense when printed in black-and-white, and remove any reference to color in the text. Only one file is accepted for each figure. Do you intend to pay to include color figures in print? If yes, please indicate which figures in the comments box.	Yes
If yes, please indicate which figures in the comments box. as follow-up to "The flat fee for including color figures in print is \$800, regardless of the number of color figures. There is no fee for online only color figures. If you decide to not print figures in color, please ensure that the color figures will also make sense when printed in black-and-white, and remove any reference to color in the text. Only one file is accepted for each figure. Do you intend to pay to include color figures in print? If yes, please indicate which figures in the comments box." "	Fig 1-3, 5-14
If there is anything else you wish to communicate to the editor of the journal, please do so in this box.	A zoom into figure 7 as well as Videos and Data (S2-S3) to illustrate and reproduce the measured dynamics are made available to the reader in the supplemental data. Captions are provided in Captions_ESM.txt

Dynamical Behaviour and Stability Analysis of Hydromechanical Gates

Fabian A. Bernhard¹ and Paolo Perona²

¹Research Engineer, CRYOS, Institute of Environmental Engineering, School of Architecture, Civil and Environmental Engineering, EPFL, Lausanne, CH. Email: fabian.bernhard@alumni.epfl.ch

²Professor, Chair of Environmental Engineering, Institute for Infrastructure and Environment, School of Engineering, University of Edinburgh, UK. Email: paolo.perona@ed.ac.uk

ABSTRACT

This study revisits the stability of hydromechanical gates for upstream water surface regulation, also known as AMIL gates. AMIL gates are used in irrigation canals, where they are often installed in series. From the regulation perspective, instabilities are undesired, as they generate waves and fluctuations in the discharge. We describe a mathematical model for an AMIL gate as a nonlinear dynamical system, which permits to analyse the dynamic interaction between the local water level and the gate position. The feedback effect of the gate on the water level is introduced by considering a storage volume of length l . In the derived model, waves are simplified to fluctuations of the flat water surface of the storage volume. Although previous studies used the same model, none has clarified the sensitivity of the model to the parameter l . The role of this parameter is investigated and it is calibrated with experimental measurements. The precision of the regulation is described by the *decrement*, the range of the water level around the target level. Based on the mathematical model, a relationship for calibration of the gate and precision of regulation is presented. The subsequent stability analysis of the dynamical system focuses on five control parameters and sheds light on their influence on the gate behaviour. Hopf bifurcations are identified, which separate stable equilibrium solutions from stable periodic solutions. Further work might consider the implications of the periodic solutions on gates that work in series, as well as envision the innovative use of such gates outside of the domain of irrigation canals to obtain dynamic environmental flows in hydropower systems.

INTRODUCTION

Hydromechanical gates for upstream water surface regulation, also known as AMIL gates, are used in gravity irrigation systems to control water levels upstream of their location for varying flow rates in the main canal (Rogers and Goussard 1998; Ramirez-Luna 1997; Montañés 2005; GEC Alstom 1992). This flow rate may vary if the inflow upstream changes or as water is removed via lateral off-takes from the main canal according to a varying demand.

AMIL gates are a specific type of radial gates, used as automatic control structures in order to cope with these variations in flow rate by opening or closing in response to the current water level. Their objective is to maintain the

30 water level in a certain range around their trunnion axis. This range is referred to as *decrement* (Ramirez-Luna 1997;
31 GEC Alsthom 1992) and can be related to the gate properties (calibration of mass and centre of gravity).

32 A photo and an illustration of an AMIL gate are shown in figures 1 and 2. In addition to typical radial gates, they
33 are equipped with a toroidal float attached to the upstream side of the gate leaf, counterweights on the downstream
34 side, and a damping device to reduce oscillations. As the gate is operated only by the water force, AMIL gates are
35 counted among the *hydromechanical* gates (Cassan et al. 2011).

36 Through the interaction of the gate and the local water level, oscillations are possible and are indeed observed,
37 particularly when the damping element (see ahead) is worn out (Ramirez-Luna 1997; Montañés 2005) (and Bernhard,
38 2015, unpublished; available by contacting the authors). Fig. 1 and two videos in the supplementary material show
39 an aged experimental AMIL gate at École Polytechnique Fédérale de Lausanne in Switzerland (EPFL) that exhibits an
40 oscillating behaviour. This behaviour was triggered by operation of the lateral off-take structures in the foreground of
41 the photo. We can see a wave propagating in the upstream direction. Waves, and thus oscillating behaviour in general,
42 are undesired as they are likely to affect the discharges in the main canal and the lateral off-takes.

43 A number of other authors have investigated instabilities related to gate operation in irrigation canals in general or
44 more specifically instabilities of AMIL gates.

45 Litrico et al. (2007) developed a general method for stability analysis of automatic gates in open-channels. The
46 Saint-Venant equations (1D shallow water equations) for the open-channel dynamics were combined with a model of
47 the automatic gate in order to derive the governing equations. The method was based on linearisation and Laplace
48 transform of these governing equations. To simplify, only a static relationship between the gate opening and the water
49 level was assumed, i.e. the gate is in equilibrium with the water level at each instant. This was based on the assumption
50 that gate dynamics are negligible in front of the pools dynamics. Litrico and Fromion (2009) used a similar approach
51 also throughout (Litrico and Fromion 2009).

52 Stability of AMIL gates was specifically investigated in (Corriga et al. 1977; Corriga et al. 1980; Ramirez-Luna
53 1997). Corriga et al. (1977) investigated an AMIL gate connected to a short, level pool and considered a dynamic
54 interaction between the gate position and the water level. A calibration of the gate, that results in zero total decrement,
55 was implicitly assumed. The model was linearised and the step responses of the linear and the nonlinear systems were
56 compared. By means of the Laplace transform, a transfer function of the linear system was derived. Instabilities were
57 discovered and their existence was related to the value of the damping parameter. However, no study on the influence
58 of the choice of the level pool length was done. This seems to be an important problem to address, given that the level
59 pool is a simplifying assumption based on a model-related – not problem related – parameter.

60 Corriga et al. (1980) considered two long canals connected by an AMIL gate. The Saint-Venant equations were
61 used for the canals and the gate was modelled with an adaptation of the model developed in (Corriga et al. 1977).
62 The adaptation included the assumption of a static gate. The system was identified to be unconditionally stable for

63 subcritical flows.

64 Ramirez-Luna (1997) applied the approach that was later described in (Litrico et al. 2007) to three different
65 hydromechanical gate types including AMIL gates. The findings for AMIL gates were also reported in (Ramirez-Luna
66 et al. 1998). The angular moment exerted by the water on the gate was based on (Corriga et al. 1977), but it was refined
67 by taking into account the decrement. Canal hydrodynamics were then modelled using the Saint-Venant equations.
68 When connected to a canal, the gates were also assumed to be in a static equilibrium, based on the different time
69 scales of the gates and canals considered in the study. Coupling of a single canal to an AMIL gate was determined
70 to be unconditionally stable, while coupling of multiple canal reaches with AMIL gates were identified to be possibly
71 unstable. For the latter case, a stability criterion was developed. These instabilities, however, were not attributed to the
72 coupling of a canal reach to an AMIL gate, but rather to the interaction between canal reaches through waves.

73 Above overview shows that in most of the previous studies (apart from (Corriga et al. 1977)) the gate was assumed
74 to be in static equilibrium with the current water level. The time scale of the gate dynamics were assumed to be much
75 shorter than the dynamics of canal reaches in typical irrigation networks. The gate dynamics were thus neglected and
76 the gate's purpose consisted only in determining the boundary conditions for the water level and the discharge based
77 on the static equilibrium law (illustrated further on by Fig. 4).

78 However, observed wave formation through gate oscillation suggest that, on a local spatial scale of the order of the
79 generated surface perturbations, the dynamics of a gate and a canal can be of similar time scales. (Wave formation
80 was observed for example at an experimental gate at EPFL and is shown in Fig. 1 and by two videos provided as
81 supplementary material.) A dynamic gate-water level relation seems required in order to characterise the dynamics
82 of the instability and to envision the use of such gates outside of irrigation canals, e.g. to generate non-proportional
83 releases at water intakes (Razurel et al. 2015; Gorla and Perona 2013). We adopt an approach similar to the one in
84 (Corriga et al. 1977), but differing in some basic aspects. We use a model that allows for a decrement (by considering
85 an arbitrary position for the centre of gravity as in (Ramirez-Luna 1997)) and also distinguish between submerged and
86 free flowing discharge of the gate. The gate response to perturbations depends on various gate parameters and can be
87 investigated with a stability analysis. We investigate systematically the influence of the level pool length l as well as
88 the other model parameters (damping, discharge, and decrement). Lyapunov and asymptotic stability theory is used
89 in order to determine the parameter domains in which instabilities might occur. Besides using linearised methods we
90 attempt a characterisation of the nonlinear system.

91 This article can be outlined as follows. In section 2 the technical description and the dimensionless gate parameters
92 are presented. Then, in section 3 we derive the mathematical model describing the dynamics and expose the relationship
93 between the decrement and the calibration, that can be attained by altering the position of the centre of gravity using
94 the counterweights. In section 4 we then assess the stability of the derived system with respect to various control
95 parameters. In section 5 the model is calibrated to two observed dynamic behaviours of the EPFL gate.

TECHNICAL GATE DESCRIPTION AND DIMENSIONLESS GEOMETRY

An AMIL gate in a trapezoidal canal can be characterised by the geometrical quantities shown in Fig. 2.

Gate dimensions are described by: gate axis height Y_a ; gate radius R ; float radius r ; bottom width of gate leaf b ; top width of gate leaf D ; width of float b_F .

The float is of constant width and thickness and corresponds thus to a toroid with a rectangular cross section of side lengths b_F and $(r - R)$. The width of the float is assumed to be a fraction of the canal width at the bottom ($b_F/b = 0.8$).

The gate position is given by θ , which is defined as the angle between the horizontal line and the lower part of the float. Other angles are: extension of gate leaf below float ω_F ; position of centre of gravity in polar coordinates ω_{CG} and r_{CG} . The position of the closed gate can be expressed using above quantities as

$$\theta_c = \arcsin(Y_a/R) - \omega_F. \quad (1)$$

The canal is characterised by: bottom width b ; side slope of trapezoidal canal wall α .

Vertical heights are defined as: upstream, *controlled* water level Y_1 , which is the target of the regulation; downstream water level Y_3 ; vertical opening of gate Y_g (not shown). The gate opening can be expressed as

$$Y_g = Y_a - R \sin(\theta + \omega_F). \quad (2)$$

Further quantities are needed to define the model that we develop in section 3. For the conservation of angular momentum we will refer to: angular damping coefficient c_ω ; moment of inertia of movable parts of the gate about the gate axis I . We also consider a volume of water in front of the gate of length l . In- and outflow of this volume are designated by Q_i and Q_g . To express the gate discharge Q_g , a discharge coefficient μ is used, combining the effect of the contraction and velocity coefficient (C_c and C_v). Note that we neglect the slope of the canal bottom at the gate.

Brochures by gate manufacturers indicate 21 typical gate sizes with varying geometries (e.g. see (GEC Alsthom 1992)). These 21 sizes can be grouped into four classes with distinct dimensionless characteristics. By using the top width of the gate leaf D as scaling, we define dimensionless length parameters as follows

$$\tilde{Y}_a = \frac{Y_a}{D} \quad \tilde{b} = \frac{b}{D} \quad \tilde{R} = \frac{R}{D} \quad \tilde{r} = \frac{r}{D}. \quad (3)$$

The dimensionless gate parameters of these typical sizes are shown in Fig. 3 and the group averages are shown in table 1. Table 1 shows additionally the values of the gate used in (Corriga et al. 1977). To facilitate comparison we base our stability investigations on the same gate. (The gate in (Corriga et al. 1977) is based on $D = 3.95\text{m}$, $I = 4500\text{Nms}^2/\text{rad}$, $c_\omega = 20000\text{Nms}/\text{rad}$, and $l = 1\text{m}$.)

MATHEMATICAL MODELLING

AMIL Gate as a Dynamical System

In the following, the dynamical system description of an AMIL gate in a trapezoidal canal is derived.

Gate Movement

To determine the gate movement, we follow closely Corrigan et al. (1977, Ramirez-Luna (1997) and consider the moments on the gate acting about the gate axis

$$I \frac{d^2\theta}{dt^2} + c_\omega \frac{d\theta}{dt} = M_w(\theta, Y_1) + M_g(\theta). \quad (4)$$

We refer with M_w respectively M_g to the moments exerted by the water respectively by gravity on the gate (the sign is defined by the direction of θ , i.e positive sign of M in the direction of closing gate). As third moment, we consider the effect of the angular damping coefficient c_ω .

The moment by gravity M_g depends on the position of the centre of gravity (ω_{CG}, r_{CG}) and the mass m of the movable parts of the gate. Referring to Fig. 2 we can write

$$M_g(\theta) = -mr_{CG}g \cos(\theta + \omega_{CG}). \quad (5)$$

To compute the moment due to the water, we simplify by assuming a hydrostatic pressure distribution along the gate leaf based on the water level Y_1 . In doing so we follow (Corrigan et al. 1977; Ramirez-Luna 1997). Preliminary investigations (Bernhard, 2015, unpublished; available by contacting the authors) compared the hydrostatic model to a model based on conservation of momentum over a control volume. The simpler hydrostatic model was able to reproduce more faithfully measured equilibrium positions of the EPFL gate as well as Computational Fluid Dynamics (CFD) simulations for three different gate positions. Hence, we neglect non-hydrostatic effects. As AMIL gates are radial gates and have a radial float with a curvature centred in the gate axis, the water pressure on the gate leaf and curved float surface does not exert a moment about the gate axis. We furthermore assume that any water mass on the downstream side of the gate doesn't exert any moment either. Thus, it is sufficient to consider only the bottom part of the float for the moment due to the water. We can express the hydrostatic pressure p as a function of θ and Y_1 and the distance \hat{r} to the gate axis

$$p(\hat{r}, \theta, Y_1) = \rho g (Y_1 - (Y_a - \sin(\theta)\hat{r})), \quad (6)$$

and integrate the moment about the gate axis over the float bottom. This leads to the expression for the moment exerted

by the water (7)

$$M_w(\theta, Y_1) = -b_F \int_R^r \hat{r} p(\hat{r}, \theta) d\hat{r} \quad (7)$$

$$= -b_F \rho g \left(\frac{r^2 - R^2}{2} (Y_1 - Y_a) + \frac{r^3 - R^3}{3} \sin(\theta) \right). \quad (8)$$

148 The angular damping coefficient is assumed to be constant, although the elongation of the dashpot used for damping
 149 depends on the current gate position. The reader might refer to (Ramirez-Luna 1997), where this nonlinear effect is
 150 further treated. To include it, additional parameters describing the exact attachment configuration would need to be
 151 defined. However, when using the parameters given by (Ramirez-Luna 1997), the nonlinear effect remains small as
 152 shown recently (Bernhard, 2015, unpublished; available by contacting the authors) and it will therefore be neglected
 153 in this study by using a constant angular damping coefficient.

154 *Water Level Change*

155 Modelling a level pool allows dynamic interaction between the gate position and the water level. This level pool
 156 acts as a finite control volume for mass conservation of an incompressible fluid (Munson et al. 2009). It allows to
 157 transform the effect of a change in the gate position via a change in discharge into a change in the water level. Note that
 158 a level pool represents a simplification of reality and that the length we choose for this reservoir is a model parameter
 159 that can be linked to reality for example through calibration.

160 Considering a length l , the level pool leads to a volume

$$161 \quad V = b l Y_1 + \tan(\alpha) l Y_1^2. \quad (9)$$

162 Note that only the volume in front of the gate is considered (between the first two dashed, red lines in Fig. 2) and that
 163 the volume below the gate is approximated with a constant value regardless of the gate position. Change in the level
 164 pool volume is related to the in- and outflow by a simple reservoir volume balance equation

$$165 \quad \frac{dV}{dt} = Q_i - Q_g, \quad (10)$$

166 or, in terms of water level Y_1 by using (9)

$$167 \quad \frac{dY_1}{dt} = \frac{1}{l(b + 2 \tan(\alpha) Y_1)} (Q_i - Q_g). \quad (11)$$

Discharge Through the Gate

The flow rate or *discharge* through the gate needs to be expressed as a function of Y_1 , θ , and Y_3 . We distinguish between free and submerged flow depending on the downstream water depth. In case of free flow we replace Y_3 with $C_c Y_g$, which represents the depth of the vena contracta.

The discharge law and coefficients we use are based on (Corrigan et al. 1977). The law computes the total discharge as a sum of an orifice flow and free weir discharge by considering two distinct areas $\sigma_{orifice}$ and σ_{free} . These areas are shown for the free flowing gate in Fig. 2 and they represent the unobstructed areas between the canal bottom and the downstream depth Y_3 ($\sigma_{orifice}$), respectively between the downstream depth Y_3 and the upstream depth Y_1 (σ_{free}). For simplicity, the same correction factor μ is used for both these discharges, similar to (Corrigan et al. 1977). To express the discharge over each area we make the common assumptions of horizontal flow, atmospheric pressure within the weir nappe, as well as uniform and small approaching velocity upstream of the gate (Munson et al. 2009). We write the discharge as

$$Q = \int_0^{Y_1} u(\hat{y})b(\hat{y})d\hat{y}. \quad (12)$$

To express the discharges for the two distinct areas with the problem parameters, we need to distinguish between the cases $Y_3 > Y_g$ (submerged) and $Y_3 < Y_g$ (e.g. free flow), where $Y_g = Y_g(\theta)$ refers to the gate opening from equation (2).

For $Y_3 < Y_g$ (e.g. for free flow $Y_3 = C_c Y_g$) we decompose the total discharge in an orifice part: Q_1 , a free weir part through the area below Y_g : Q_2 , and a free weir part through the area on the side of the gate: Q_3 . This leads to

$$Q_g = Q_{g,free} = Q_1 + Q_2 + Q_3, \quad (13)$$

where

$$Q_1 = \mu\sqrt{2g} (Y_3(b + \tan(\alpha)Y_3)) \sqrt{Y_1 - Y_3} \quad (14a)$$

$$Q_2 = \mu\sqrt{2g} \left[\frac{2}{3} b((Y_1 - Y_3)^{3/2} - (Y_1 - Y_g)^{3/2}) + \frac{4}{15} \tan(\alpha) \left((3Y_3 + 2Y_1)(Y_1 - Y_3)^{3/2} - (3Y_g + 2Y_1)(Y_1 - Y_g)^{3/2} \right) \right] \quad (14b)$$

$$Q_3 = \mu\sqrt{2g} \left(\frac{2}{3} 2 \tan(\alpha) Y_g (Y_1 - Y_g) \right) \sqrt{Y_1 - Y_g}. \quad (14c)$$

For $Y_3 > Y_g$ (submerged case) we follow (Corrigan et al. 1977) and write

$$Q_g = Q_{g,submerged} = \mu\sqrt{2g} (\sigma_{orifice} + \frac{2}{3} \sigma_{free}) \sqrt{Y_1 - Y_3}, \quad (15)$$

where

$$\sigma_{orifice} = bY_g + Y_g^2 \tan(\alpha) + 2Y_g \tan(\alpha)(Y_3 - Y_g) \quad (16a)$$

$$\sigma_{free} = 2Y_g \tan(\alpha)(Y_1 - Y_3). \quad (16b)$$

Corrigan et al. (1977) modelled submerged conditions with a varying downstream depth, based on the discharge itself. The applied formulation does not always yield physical solutions, especially for low discharges at almost closed gate. For submerged conditions, we impose therefore a *fixed* downstream depth, independent from the flow rate, and consider the free flowing gate separately.

Next, we normalise the input discharge by introducing a hypothetical nominal discharge Q_n as a scaling

$$Q'_i = \frac{Q_i}{Q_n}. \quad (17)$$

For both, free and submerged gates, we define the nominal discharge as the free discharge at completely open gate with the water level at axis height, i.e.

$$Q_n := Q_{g,free}(\theta = 0, Y_1 = Y_a, Y_3 = C_c Y_g). \quad (18)$$

Combined system and nondimensionalisation

Combining the derived models for the variation of the gate position (4) and water level (11), we can derive a dynamical system governed by the following basic equations

$$\begin{aligned} \frac{d^2\theta}{dt^2} = & -\frac{c_\omega}{I} \frac{d\theta}{dt} \\ & + \frac{1}{I} \left[-b_F \rho g \left(\frac{r^2 - R^2}{2} (Y_1 - Y_a) + \frac{r^3 - R^3}{3} \sin(\theta) \right) \right. \\ & \left. - m r_{CG} g \cos(\theta + \omega_{CG}) \right] \end{aligned} \quad (19a)$$

$$\frac{dY_1}{dt} = \frac{1}{l(b + 2 \tan(\alpha) Y_1)} [Q_n Q'_i - Q_g(\theta, Y_1, Y_3)]. \quad (19b)$$

With basic algebraic manipulations we reformulate (19) as

$$\frac{d^2\theta}{dt^2} = c_1 \frac{d\theta}{dt} + c_2 (Y_1 - Y_a) + c_3 \cos(\theta) + c_4 \sin(\theta) \quad [\text{rad/s}^2] \quad (20a)$$

$$\frac{dY_1}{dt} = c_6 \frac{1}{b + 2 \tan(\alpha) Y_1} [Q_n Q'_i - Q_g(\theta, Y_1, Y_3)], \quad [\text{m/s}] \quad (20b)$$

where the definitions of the constants c_1 to c_6 are reported in appendix I.

We now derive the dimensionless form of the basic equations (20) by introducing a length scale Λ and a time scale τ , to scale all the lengths (Y, l, R, r, \dots) and time

$$Y = \Lambda \tilde{Y} \quad t = \tau \tilde{t}.$$

Based on the geometrical normalisation it is straightforward to choose $\Lambda = D$. We assume a time scale $\tau = \sqrt{\frac{D}{g}}$. Equations (20) can then be reformulated as

$$\frac{d^2\theta}{d\tilde{t}^2} = C_1 \frac{d\theta}{d\tilde{t}} + C_2(\tilde{Y}_1 - \tilde{Y}_a) + C_3 \cos(\theta) + C_4 \sin(\theta) \quad [\text{rad}^2] \quad (21a)$$

$$\frac{d\tilde{Y}_1}{d\tilde{t}} = C_6 \frac{Q_n Q'_i - Q_g(\theta, \tilde{Y}_1, \tilde{Y}_3)}{\tilde{b} + 2 \tan(\alpha) \tilde{Y}_1}, \quad [-] \quad (21b)$$

196 where the constants C_1 to C_6 in equations (21) are given in appendix I.

The system designated by equations (21) can be rewritten as three first-order equations

$$\frac{d}{d\tilde{t}} \theta_1 = \theta_2 \quad (22a)$$

$$\frac{d}{d\tilde{t}} \theta_2 = C_1 \theta_2 + C_2(\tilde{Y}_1 - \tilde{Y}_a) + C_3 \cos(\theta_1) + C_4 \sin(\theta_1) \quad (22b)$$

$$\frac{d}{d\tilde{t}} \tilde{Y}_1 = \frac{C_6}{\tilde{b} + 2 \tan(\alpha) \tilde{Y}_1} (Q_n Q'_i(\tilde{t}) - Q_g(\theta_1, \tilde{Y}_1, \tilde{Y}_3(\tilde{t}))), \quad (22c)$$

197 which is a system of the form

$$198 \quad \frac{d}{d\tilde{t}} \mathbf{x} = \mathbf{F}(\mathbf{x}, \tilde{t}), \quad (23)$$

199 with states $\mathbf{x} = (\theta_1, \theta_2, \tilde{Y}_1)^T := (\theta, \frac{d}{d\tilde{t}}\theta, \tilde{Y}_1)^T$.

200 Equations (22) characterise a three-dimensional, nonautonomous, nonlinear dynamical system. The inputs to the
201 system are $Q'_i(\tilde{t})$ and $\tilde{Y}_3(\tilde{t})$ (if submerged). By integrating system (22) it is possible to simulate a transient response to
202 time dependent inputs.

203 However, most of the stability analysis in this study is based on the assumption that the inputs are constant in time.

204 In that case, the inputs can be regarded as parameters of a completely autonomous system

$$205 \quad \frac{d}{d\tilde{t}} \mathbf{x} = \mathbf{F}(\mathbf{x}). \quad (24)$$

206 Based on equation (24) we define an equilibrium point \mathbf{x}^* such that $\mathbf{F}(\mathbf{x}^*) = 0$.

Calibration of the Gate and Control Parameters

In the following, we show how the mass of the gate and the position of the centre of gravity can be related to the decrement in \tilde{Y}_1 .

We define the decrement as the difference in the equilibrium state \tilde{Y}_1 between completely closed gate $\theta_1 = \theta_c$ ($Q'_i = 0$) and completely open gate $\theta_1 = 0$. Fig. 4 shows the equilibrium states \tilde{Y}_1^* vs. θ_1^* for various Q'_i . The figure indicates the decomposition of the total decrement into a decrement above (\tilde{d}_A) and a decrement below the gate axis (\tilde{d}_B). Given these definitions we can derive an analytical expression for ω_{CG} and $\tilde{m}r_{CG}$ as function of \tilde{d}_A and \tilde{d}_B by considering the equilibrium points at these two positions. According to the above definition of the decrement, these gate positions are in principle $\theta_{1A} = 0$ and $\theta_{1B} = \theta_c$. However, we can remain more general by using arbitrary positions $\mathbf{x}_A^* = (\theta_{1A}, 0, \tilde{Y}_a + \tilde{d}_A)^T$ and $\mathbf{x}_B^* = (\theta_{1B}, 0, \tilde{Y}_a - \tilde{d}_B)^T$. Setting equation (22b) at these positions to zero yields

$$\begin{cases} \tilde{m}r_{CG} = -\frac{(\tilde{r}^2 - \tilde{R}^2)\tilde{d}_A/2 + (\tilde{r}^3 - \tilde{R}^3)\sin(\theta_{1A})/3}{\cos(\theta_{1A} + \omega_{CG})} \\ \tilde{m}r_{CG} = -\frac{(\tilde{r}^2 - \tilde{R}^2)(-\tilde{d}_B)/2 + (\tilde{r}^3 - \tilde{R}^3)\sin(\theta_{1B})/3}{\cos(\theta_{1B} + \omega_{CG})}. \end{cases} \quad (25)$$

Considering the specific positions $\theta_{1A} = 0$ and $\theta_{1B} = \theta_c$, equation (25) simplifies eventually to

$$\begin{aligned} \tan(\omega_{CG}) &= \tan(\omega_{CG} + k\pi) \quad \forall k \in \mathbb{Z} \\ &= \frac{1}{\tan(\theta_c)} - \frac{1}{\tilde{d}_A} \frac{2(\tilde{r}^3 - \tilde{R}^3)}{3(\tilde{r}^2 - \tilde{R}^2)} + \frac{\tilde{d}_B}{\tilde{d}_A} \frac{1}{\sin(\theta_c)} \end{aligned} \quad (26)$$

Thus, an analytical expression for ω_{CG} and $\tilde{m}r_{CG}$ is given by

$$\begin{cases} \omega_{CG} = \pi + \arctan\left(\frac{1}{\tan(\theta_c)} - \frac{1}{\tilde{d}_A} \frac{2(\tilde{r}^3 - \tilde{R}^3)}{3(\tilde{r}^2 - \tilde{R}^2)} + \frac{\tilde{d}_B}{\tilde{d}_A} \frac{1}{\sin(\theta_c)}\right) \\ \tilde{m}r_{CG} = \frac{1}{\cos(\omega_{CG})} \left(-\frac{\tilde{r}^2 - \tilde{R}^2}{2} \tilde{d}_A\right). \end{cases} \quad (27)$$

Note that we assumed $\tilde{d}_A \neq 0$ to derive (25). If one imposes $\tilde{d}_A = 0$, the centre of gravity comes to lie perpendicular to the float bottom ($\omega_{CG} = \pi/2$) in order to have a balanced gate at complete opening $\theta_1 = 0$. Corrigan et al. (1977) assumed a perfectly calibrated gate, i.e. $\tilde{d}_A = \tilde{d}_B = 0$. This corresponds to the ideal case, regulating the water level without any deviation from \tilde{Y}_a . Given $\tilde{Y}_1 = \tilde{Y}_a$, the gate is in equilibrium for any position θ_1 . Under this assumption, we have $\omega_{CG} = \pi/2$, and the mass has to compensate precisely the immersed float $\tilde{m}r_{CG} = (\tilde{r}^3 - \tilde{R}^3)/3$. Therefore, the terms C_3 and C_4 become zero and the system simplifies.

The information available in (GEC Alstom 1992) indicates a typical total decrement $\tilde{d}_A + \tilde{d}_B$ of 0.02 (-). In the following analysis, we assume $\tilde{d}_B = 0$ and $\tilde{d}_A = 0.02$.

The typical functioning of the AMIL gate is illustrated by Fig. 5. A free gate, subject to a step-like increasing

227 input $Q'_i(\tilde{t})$, is simulated starting at the equilibrium state. Simulation a) shows that with the arrival of the increased
 228 discharge the gate opens and the water level rises within the limits defined by the decrement. By opening the gate the
 229 increase in water level is mitigated. We can furthermore compare the behaviour of the same gate with different damping
 230 coefficients and different level pool lengths (b) and c)). While the strongly damped gate a) follows the equilibrium
 231 curve closely, the less damped gate b) oscillates during the transition from one equilibrium point to the other. We can
 232 observe that the shorter level pool b) influences the trajectory of these oscillations as the water level rises more quickly.
 233 The observed oscillations are possible due to the assumption of a dynamic equilibrium between gate and water level,
 234 instead of a static relationship, that would simply follow the equilibrium curve.

235 Once a gate geometry and size is chosen (i.e. $\alpha, \tilde{b}, \tilde{b}_F, \tilde{Y}_a, \tilde{R}, \tilde{r}, \omega_F, \tilde{I}$) and further constants are defined ($\mu = C_c C_v$),
 236 five control parameters \mathbf{m} remain to completely define the autonomous system (24). We can recast the function \mathbf{F} to
 237 use these parameters \mathbf{m} as arguments and the system becomes

$$238 \quad \frac{d}{d\tilde{t}} \mathbf{x} = \mathbf{F}(\mathbf{x}, \mathbf{m}) \quad \mathbf{m} = \begin{bmatrix} \tilde{c}_\omega \\ Q'_i \\ \tilde{d}_A \\ \tilde{I} \\ \tilde{Y}_3 \end{bmatrix}, \quad (28)$$

239 which is the form we analyse in the following.

240 STABILITY ANALYSIS AND NONLINEAR EFFECTS OF CONTROL PARAMETERS

241 Preliminary Consideration

242 We start with investigating the two limit cases, where the level pool dynamics happen on a much faster ($\tilde{I} \ll 1$) or
 243 slower scale ($\tilde{I} \gg 1$) than the gate dynamics. Note first that the constants C_1, C_2 , and C_4 are of order $\mathcal{O}(1)$, C_3 is of
 244 order $\mathcal{O}(10^{-2})$, and C_6 is of order $\mathcal{O}(\tilde{I}^{-1})$.

For $\tilde{I} \gg 1$ ($C_6 \rightarrow 0$) we infer from equations 21 (or equations 20) that oscillations of \tilde{Y}_1 are slow and \tilde{Y}_1 can be
 considered constant. Equation 21a describes the gate movement, during which a constant value for \tilde{Y}_1 can be assumed.
 The eigenfrequency of this subsystem is given by linearising equation 21a around an equilibrium point \mathbf{x}^* (i.e. \tilde{Y}_1^* and
 θ^*) which yields:

$$245 \quad \omega_0 = \sqrt{C_3 \sin(\theta^*) - C_4 \cos(\theta^*)} \quad (29a)$$

$$\omega = \sqrt{\omega_0^2 - \left(\frac{C_1}{2}\right)^2} = \sqrt{\omega_0^2 - \left(\frac{\tilde{c}_\omega}{2}\right)^2}, \quad (29b)$$

for both the undamped (ω_0) and the damped (ω) subsystem. A critical damping $\tilde{c}_{\omega, crit}$ separates under- from

overdamped systems, when $\omega_0 < \tilde{c}_\omega/2$. Furthermore, note that when the gate is perfectly calibrated, the terms C_3 and C_4 are zero. In that case if the water level is perturbed, equation 21a doesn't allow a feedback of θ and is thus unstable.

For $\tilde{l} \ll 1$ ($C_6 \rightarrow \infty$) the evolution of \tilde{Y}_1 becomes very fast compared to the gate. Dividing equation 21a by C_6 and taking the limit of $C_6 \rightarrow \infty$, results in static relationship $\tilde{Y}_1 = f(\theta)$, which is stable.

To summarise the findings of the limit cases, we conclude that the system is generally stable for both – small and large – values of \tilde{l} . The gate and level pool subsystems can thus be regarded as interfering with each other only if their time scales are similar, i.e. in an intermediate range of \tilde{l} .

In the following analysis, we consider a base state of the control parameters \mathbf{m}_0 . Varying one parameter at the time, we observe the change in the qualitative behaviour of the solutions. Equilibrium points, their stability (Lyapunov or asymptotic), one-parameter bifurcations points and the corresponding limit cycles (including their stability) are investigated by means of a combination of analytical and numerical methods. For comparison with (Corriga et al. 1977) this analysis is based on the same gate. Besides the geometric gate properties mentioned in table 1, we use values based on either (Corriga et al. 1977): $\tilde{l} = 0.0103$, and $\mu = C_c C_v = 0.65$ ($C_c = \mu/0.97$); or from (GEC Alstom 1992): $\alpha = \arctan(1/2)$. The base set of control parameters is given by

$$\mathbf{m}_0 = \begin{bmatrix} \tilde{c}_{\omega,0} \\ Q'_{i,0} \\ \tilde{d}_{A,0} \\ \tilde{l}_0 \\ \tilde{Y}_{3,0} \end{bmatrix} = \begin{bmatrix} 1.0 \\ 0.5 \\ 0.02 \\ 0.253 \\ 0.25 \end{bmatrix}. \quad (30)$$

Influence of \tilde{c}_ω

Linear stability of equilibrium points for the parameters \mathbf{m}_0 can be studied with the eigenvalues of the Jacobian ($\frac{\partial F}{\partial \mathbf{x}}$) after linearisation (Guckenheimer and Holmes 1993). Due to the complexity of the system, only one equilibrium point is computed numerically. The eigenvalues of the Jacobian, evaluated at the equilibrium point, are shown in Fig. 6 for various values of \tilde{c}_ω for both, free and submerged gate. In both cases, we observe a single real and negative eigenvalue and a pair of complex conjugate eigenvalues. The pair of complex eigenvalues has a positive real part for low values of \tilde{c}_ω but it becomes negative above a certain limiting value. These limiting values $\tilde{c}_{\omega,lim}$ are 1.670 and 1.097 for the free respectively the submerged gate. The equilibrium point is thus unstable at the lower values, but is stabilised at the higher damping. Numerical simulations with the nonlinear system (28) using slightly perturbed initial conditions confirmed this stabilising value of \tilde{c}_ω . The eigenvalues remain in the left half-plane, i.e. stable, for further increases in the damping parameter \tilde{c}_ω . We note that above another specific value of \tilde{c}_ω the pair of complex conjugate eigenvalues becomes real valued ($\tilde{c}_{\omega,crit} = 42.0$, respectively 14.8). This critical damping value illustrates the effect

of the level pool (equation 21b), which was neglected for $\tilde{c}_{\omega,crit}$ in the preliminary considerations. The qualitative characteristics of this plot of the eigenvalues in Fig. 6 are similar to the plot of the roots of the transfer function shown in (Corriga et al. 1977).

Simultaneous passing of the imaginary axis by two eigenvalues, while no other eigenvalue has zero real part, indicates a Hopf bifurcation at the parameter value of the crossing (Guckenheimer and Holmes 1993). A Hopf bifurcation describes the emergence of limit cycles from an equilibrium point when a parameter is varied (Guckenheimer and Holmes 1993; Ermentrout 2002). We investigate this bifurcation of the nonlinear system at $\tilde{c}_{\omega,lim}$ with the software package XPPAUT (Ermentrout 2002), containing the numerical continuation software AUTO (Doedel and Oldeman 2012).

Fig. 7 shows the one-parameter bifurcation diagrams for various control parameters for the submerged system. These diagrams show the gate position θ_1 in equilibrium position respectively the minimum and maximum values on the limit cycles, as well as the periods \tilde{T} of the limit cycles. We note the emergence of stable limit cycles when the damping is below the limiting value. Having stable limit cycles, the system undergoes a *supercritical* Hopf bifurcation.

The existence of these periodic solutions is confirmed numerically. Periodic solutions, found using a boundary value approach, are shown in Fig. 8. (The applied procedure is based on (Higgins 2013), which also explicits the derivation of the boundary value problem.)

The evolution of the gate position and water level during a cycle and the trajectory in the state space are shown for the free gate (left) and the submerged gate (right) for \mathbf{m}_0 . Both systems are shown for the same damping ratios $\tilde{c}_{\omega}/\tilde{c}_{\omega,lim}$ and Q'_i is chosen for each system separately to yield similar equilibrium positions in θ_1 . The trajectories are in agreement with the values shown by Fig. 7. We observe a phase shift in the trajectories between gate position θ_1 and water level \tilde{Y}_1 . The periods and Floquet multipliers of these periodic solutions are shown in table 2. With only one Floquet multiplier of magnitude 1 or higher, the limit cycles are stable.

Influence of Q'_i

To assess the influence of the parameter Q'_i we first look at the linear stability of the equilibrium point for the base parameters \mathbf{m}_0 . The eigenvalues of the Jacobian are shown in Fig. 9 for various values of Q'_i for the submerged gate. The free gate is not shown, behaving qualitatively similar. As the equilibrium point depends on the value of Q'_i , the Jacobian needs to be re-evaluated at each (numerically found) equilibrium point. Again, there exists a limiting value $Q'_{i,lim}$ of 0.5638 (respectively 0.8217 for the free gate) stabilising the system. Again, numerical simulations with perturbed initial conditions confirmed these limiting values.

The evolution of the eigenvalues in the complex plane for varying Q'_i is similar to the evolution for varying \tilde{c}_{ω} . A supercritical Hopf bifurcation for the parameter Q'_i is expected and confirmed by the second bifurcation diagram in Fig. 7.

The resulting periodic solutions for values below $Q'_{i,lim}$ are qualitatively similar to the ones shown in Fig. 8 for variations in \tilde{c}_ω . The magnitude of the oscillations increase with decreasing Q'_i , an observation that can readily be inferred from the bifurcation diagram.

The response to the step-like input $Q'_i(t)$ shown in Fig. 5 illustrates the change in stability due to Q'_i . Fig. 10 compares the response to such a step-like input for the free and submerged gate using the same damping ratio $\tilde{c}_\omega/\tilde{c}_{\omega,lim} = 0.61$, based on $\tilde{c}_{\omega,lim}$ for the initial value of Q'_i . The input $Q'_i(\tilde{t})$ increases from 0.2 to 0.7. Both gates are unstable at the initial value of Q'_i and start to oscillate. The systems stabilise with increasing discharge as they are stable at the final value of Q'_i . The damping \tilde{c}_ω of the submerged gate used for the simulation is lower compared to the free gate (1.80 vs. 1.17).

Influence of \tilde{d}_A and \tilde{Y}_3

The relationship between Q'_i and $\tilde{c}_{\omega,lim}$ is illustrated by Fig. 11. It shows the free gate system using various values for \tilde{d}_A in a), while the submerged gate system uses $\tilde{d}_{A,0} = 0.02$ but various submergence depths \tilde{Y}_3 in b). Generally, the limiting values $\tilde{c}_{\omega,lim}$ decrease with increasing discharge (i.e. larger gate openings), illustrating again the stabilising effect of large Q'_i . A shift in the x -axis can be observed between the plots showing the limiting values for the same system, but either using Q'_i or θ_{eq} (compare for example subplots b) and d)). These shifts depend on the value of \tilde{d}_A or \tilde{Y}_3 . This is caused by the influence of these parameters on the equilibrium position θ_{eq} for the same Q'_i .

An increase in the decrement \tilde{d}_A might have a stabilising or destabilising effect on the system, i.e. requiring a lower/higher damping, depending on the Q'_i considered. However, the destabilising effect seems to be explained through the change in the equilibrium position θ_{eq} for different decrements. Indeed judging only by the free gate plot against θ_{eq} in c), an increase in the decrement decreases the $\tilde{c}_{\omega,lim}$ for almost all equilibrium positions.

For the submerged gate, an increase in the downstream depth \tilde{Y}_3 stabilises the gate. It is likely that this is caused by the reduced sensitivity of the gate discharge Q_g to the gate position θ_1 (i.e. a smaller $\frac{\partial Q_g}{\partial \theta}$). This can be observed for the various values of \tilde{Y}_3 in Fig. 11 (subplots b) and d)).

Influence of \tilde{l}

Already highlighted by the preliminary considerations, the system is generally stable in the limits $\tilde{l} \ll 1$ and $\tilde{l} \gg 1$, unless the total decrement is set to zero, where stability occurs only in the lower limit $\tilde{l} \ll 1$. These observations are confirmed by Fig. 12, showing the real part of the second eigenvalue of the linearised system as a function of \tilde{l} . The bifurcation diagram for \tilde{l} in Fig. 7 identifies two supercritical bifurcations. The period of the limit cycle, shown in the same figure, differs strongly.

Fig. 13 shows the identified limiting damping parameter $\tilde{c}_{\omega,lim}$ as a function of \tilde{l} . We notice that the value of \tilde{l} resulting in the highest $\tilde{c}_{\omega,lim}$ depends on the value of \tilde{d}_A .

PRACTICAL CALIBRATION OF MODEL PARAMETER \tilde{L} TO MEASURED DYNAMICS

We recall that the level surface is a simplifying assumption, using a model-related – not problem-related – parameter \tilde{L} . In the following, we calibrate this parameter \tilde{L} to observed wave interactions with a canal. We performed video measurements of the dynamical behaviour of the experimental gate at EPFL. Two distinct dynamic regimes have been recorded. Videos of the two behaviours are available as electronic supplementary material (S2 and S3). The gate position during the two dynamic responses is shown in Fig. 14.

In behaviour A), the upper end of the canal reach upstream of the gate, situated at a distance L , acts as a reflecting boundary for incoming waves. A periodic solution develops as the waves in the canal and the gate synchronise. The periodic solution corresponds to a standing wave in the canal with the gate oscillating at the same frequency.

Behaviour B) corresponds to a transient response, describing the gate rising, after being initially locked in closed position. Over the short period of time we consider, the reflecting upstream boundary has no effect on the gate, as the perturbations generated by the gate travel with a finite speed.

Both measurements were taken under free flowing conditions. The gate setup at EPFL is described by the following measured quantities: $D = 0.81\text{m}$, $R = 0.63\text{m}$, $r = 0.685\text{m}$, $Y_a = 0.367\text{m}$, $b = 0.46\text{m}$, $b_F = 0.36\text{m}$, $\omega_F = 0.173\text{m}/R$, $\alpha = \arctan(1/2)$, $\omega_{CG} = 1.61\text{rad}$, $mr_{CG} = 8.13\text{kgm}$, and the estimated dynamic properties: $I = 7.67\text{Nms}^2/\text{rad}$, and $c_\omega = 69.0\text{Nms}/\text{rad}$. The canal reach ends at a distance $L = 4.17\text{m}$ upstream of the gate leaf in a boundary, where the inflow enters the canal reach through the bottom part.

The length of the level pool volume can be calibrated to reproduce the observed behaviour. While situation A) is representative of a short canal reach under the influence of an upstream reflecting boundary, situation B) can describe an infinitely long canal reach, where the generated perturbations are not reflected upstream. These two situations can be characterised by two different values of \tilde{L} .

For behaviour A), we can describe the standing wave in the canal with standing wave theory (SWT). We recall the sensitivity of the frequency of the gate to the model parameter \tilde{L} , observed in the bifurcation diagram (Fig. 7). This allows us to estimate \tilde{L} for a given frequency. We combine both of these approaches to estimate the parameter \tilde{L} for AMIL gates with canals of various lengths L showing standing wave behaviour.

In the observed case, the ratio of the flow velocity to the wave celerity is small ($U_0/c \ll 1$). Therefore, we apply classic SWT using a constant celerity in both directions. SWT allows us to determine the frequency of a specific mode for a canal of a given length L . Based on that the parameter \tilde{L} can be determined by adjusting the frequency of the gate to the standing wave in the canal. In behaviour A) both ends of the canal were antinodes, i.e. the amplitude of the oscillations is at its maximum. This can be translated to boundary conditions prescribing the gradient of the water level to be zero. The frequency of the modes is then given by $f_n = nc/(2L)$, where the wave celerity is related to the equilibrium water level by $c = \sqrt{gY_1^*}$. The observed behaviour A) corresponds to the mode with $n = 4$, giving us a theoretical frequency by wave theory of $f_{4,SWT} = 0.93\text{Hz}$ or $\omega_{4,SWT} = 5.85\text{rad/s}$ (using $Y_1^* = 0.385\text{m}$ for both). The

369 level pool length required to obtain the same frequency of gate oscillations is $\tilde{l}_{SWT} = 0.043$.

370 However, the frequency of the observed behaviour does not exactly coincide with the one predicted by standing
371 wave theory. Further studies including nonlinear effects may explain such differences. The measured frequency was
372 $f_{meas} = 0.81\text{Hz}$ or $\omega_{meas} = 5.09\text{rad/s}$. The level pool length corresponding to this frequency is $\tilde{l}_{meas,A} = 0.05$.

373 We consider behaviour B) over roughly two oscillation cycles, corresponding to the time before the perturbations
374 return. (The inflow Q_i was adapted to compensate the flow above the gate that occurred during the measurement.) A
375 parameter $\tilde{l}_{meas,B} = 0.14$ was calibrated for this behaviour. Transient effects from the reflection of the waves remain
376 after the two oscillations cycles, but eventually the gate stabilises.

377 The model simulation for the parameters $\tilde{l}_{meas,A}$ and $\tilde{l}_{meas,B}$ and two different inflow discharges are superimposed
378 onto Fig. 14. Note that using the value of $\tilde{l} = 0.253$ from (Corrigan et al. 1977) would result in too low frequencies to
379 reproduce either behaviour A) nor B).

380 In conclusion the choice of \tilde{l} thus depends on the type of dynamic one wants to reproduce.

381 CONCLUSION AND OUTLOOK

382 In this article a mathematical model was developed based on (Corrigan et al. 1977; Ramirez-Luna 1997) and
383 investigated with respect to various control parameters. The model was used to reproduce two kinds of dynamic
384 behaviour of an experimental gate. For the calibration of the counterweights, we presented an analytical formula
385 permitting to impose a specified decrement. The stability analysis allowed to determine limiting values for the
386 damping parameter $\tilde{c}_{\omega,lim}$. We've shown a change in behaviour at these limiting values from stable equilibria to stable
387 periodic solutions – a supercritical Hopf bifurcation. The periodic solutions are not desired in irrigation canals, leading
388 to fluctuations of discharges in the main canal and lateral off-takes. The constant inflow parameter Q'_i exhibits similar
389 influence on the system as $\tilde{c}_{\omega,lim}$.

390 The identified limiting values depend on the model parameter \tilde{l} . It is therefore important to use a representative
391 level pool length \tilde{l} or to simply select the most conservative damping $\tilde{c}_{\omega,lim}$ among the estimates obtained with a wide
392 range of \tilde{l} .

393 In view of the typically slow canal dynamics in irrigation canal networks (Corrigan et al. 1980; Ramirez-Luna
394 1997), the dynamic interactions between the water level and the gate are considered negligible by other authors and
395 the simplification of a static gate appropriate. On the other hand, the model based on a level pool, used throughout
396 this work, allows to consider the dynamic interaction between the local water level and the AMIL gate. This dynamic
397 interplay might become more important under circumstances where faster water level dynamics are present (e.g.
398 irrigations canals exhibiting resonance behaviour or situations outside of irrigation canals). Refraining from the static
399 gate simplification, by using the level pool model, seems more appropriate in those circumstances.

400 To complement existing studies (e.g. (Ramirez-Luna 1997)), the model developed here can suggest a different

401 approach to study interaction of AMIL gates installed in series. In canals exhibiting strong resonance behaviour and
 402 weak wave attenuation, waves generated by a non-static gate-water level relationship – possible to model with the
 403 derived system – might reach and influence other AMIL gates up- or downstream.

404 To operate run-of-the-river hydropower plants, non-proportional water distribution from rivers is an efficient
 405 alternative to fixed-percentage (proportional) releases of the incoming flow (Razurel et al. 2015; Gorla and Perona
 406 2013; Perona et al. 2013). AMIL gates might constitute a possible, energy-free means for this repartitioning. We
 407 envision that the combination of a weir in the river and an AMIL gate with an adapted float form in the derived canal
 408 might allow to implement non-proportional dynamic environmental flows, hence the importance of similar studies that
 409 address stability conditions.

410 APPENDIX I. CONSTANTS

411 Constants for Dimensional System

$$c_1 = -\frac{c_\omega}{I} \quad [\text{s}^{-1}] \quad (31\text{a})$$

$$c_2 = -\frac{b_F \rho g}{I} \frac{r^2 - R^2}{2} \quad [\text{rad}/(\text{s}^2\text{m})] \quad (31\text{b})$$

$$c_3 = -\frac{b_F \rho g}{I} \frac{mr_{CG}}{b_F \rho} \cos(\omega_{CG}) \quad [\text{rad}/\text{s}^2] \quad (31\text{c})$$

$$c_4 = -\frac{b_F \rho g}{I} \left(\frac{r^3 - R^3}{3} - \frac{mr_{CG}}{b_F \rho} \sin(\omega_{CG}) \right) \quad [\text{rad}/\text{s}^2] \quad (31\text{d})$$

$$c_6 = \frac{1}{l} \quad [\text{m}^{-1}] \quad (31\text{e})$$

$$(31\text{f})$$

412 Constants for Dimensionless System

$$C_1 = c_1 \tau = \tilde{c}_\omega = \frac{c_\omega}{I} \sqrt{\frac{\Lambda}{g}} \quad [-] \quad (32\text{a})$$

$$C_2 = c_2 \tau^2 \Lambda = -\frac{1}{\tilde{l}} \frac{\tilde{r}^2 - \tilde{R}^2}{2} \quad [\text{rad}] \quad (32\text{b})$$

$$C_3 = c_3 \tau^2 = -\frac{1}{\tilde{l}} \tilde{m} \tilde{r}_{CG} \cos(\omega_{CG}) \quad [\text{rad}] \quad (32\text{c})$$

$$C_4 = c_4 \tau^2 = -\frac{1}{\tilde{l}} \left(\frac{\tilde{r}^3 - \tilde{R}^3}{3} - \tilde{m} \tilde{r}_{CG} \sin(\omega_{CG}) \right) \quad [\text{rad}] \quad (32\text{d})$$

$$C_6 = \frac{\tau}{\Lambda} \frac{c_6}{\Lambda} = \frac{1}{\sqrt{g} \Lambda^{5/2}} \frac{1}{\tilde{l}} \quad [\text{s}/\text{m}^3] \quad (32\text{e})$$

$$\tilde{c}_\omega = \frac{c_\omega}{I} \sqrt{\frac{\Lambda}{g}} \quad [-] \quad (33a)$$

$$\tilde{I} = \frac{I}{\rho \tilde{b}_F \Lambda^5} \quad [\text{rad}^{-1}] \quad (33b)$$

$$\tilde{m}r_{CG} = \frac{mr_{CG}}{\tilde{b}_F \rho \Lambda^4} \quad [-] \quad (33c)$$

APPENDIX II. ACKNOWLEDGMENTS

The Swiss National Science Foundation is greatly acknowledged for funding the projects REMEDY (Grant No. PP00P2153028/1). Paolo Perona wishes to thank the Climatology Research Group at the Institute of Geography of the University of Bern for hosting him as academic guest.

APPENDIX III. SUPPLEMENTAL DATA

Fig. S1 and Videos S2-S3 with the corresponding Data S2-S3 are available online in the ASCE Library (ascelibrary.org).

REFERENCES

- Cassan, L., Baume, J.-P., Belaud, G., Litrico, X., Malaterre, P.-O., and Ribot-Bruno, J. (2011). “Hydraulic modeling of a mixed water level control hydromechanical gate.” *Journal of Irrigation and Drainage Engineering*, 137(7), 446–453.
- Corriga, G., Patta, F., Tola, S., and Usai, G. (1977). “La dinamica delle paratoie autolivellanti nelle reti di distribuzione a pelo libero [reti di irrigazione].” *Idrotecnica*, 249–255.
- Corriga, G., Sanna, S., and Usai, G. (1980). “Frequency response and dynamic behaviour of canal networks with self-levelling gates.” *Applied Mathematical Modelling*, 4(2), 125–129.
- Doedel, E. and Oldeman, B. (2012). “Auto-07p: Continuation and bifurcation software for ordinary differential equations, <<http://indy.cs.concordia.ca/auto/> and <http://www.dam.brown.edu/people/sandsted/auto/auto07p.pdf>> (Nov. 14, 2015). Department of Computer Science, Concordia University, Montreal, Canada.
- Ermentrout, B. (2002). *Simulating, analyzing, and animating dynamical systems*. Society for Industrial and Applied Mathematics.
- GEC Alsthom (1992). “Amil gates - constant upstream level control in reservoirs and canals.” *A 65 01 A - Advertisement Brochure*, <http://www.canari.free.fr/papers/neyrpic_amil_gb.tif or http://www.canari.free.fr/papers/neyrpic_amil_fr.pdf> (Nov. 14, 2015).
- Gorla, L. and Perona, P. (2013). “On quantifying ecologically sustainable flow releases in a diverted river reach.” *Journal of Hydrology*, 489, 98–107.

438 Guckenheimer, J. and Holmes, P. (1993). Nonlinear oscillations, dynamical systems, and bifurcations of vector fields.
439 Applied mathematical sciences. Springer, New York.

440 Higgins, B. G. (2013). “Stability analysis of periodic solutions, <[https://sites.google.com/site/](https://sites.google.com/site/chemengwithmathematica/home/numerical-methods)
441 [chemengwithmathematica/home/numerical-methods](https://sites.google.com/site/chemengwithmathematica/home/numerical-methods)> (Nov. 14, 2015).

442 Litrico, X., Belaud, G., and Fromion, V. (2007). “Stability analysis of automatic water level control gates in open-
443 channels.” 46th IEEE Conference on Decision and Control, 2007, IEEE, 1591–1596.

444 Litrico, X. and Fromion, V. (2009). Modeling and control of hydrosystems. Springer London.

445 Montañés, J. L. (2005). Hydraulic canals: design, construction, regulation and maintenance. Taylor & Francis, London.

446 Munson, B. R., Young, D. F., Okiishi, T. H., and Huebsch, W. W. (2009). Fundamentals of fluid mechanics. John Wiley.

447 Perona, P., Dürrenmatt, D. J., and Characklis, G. W. (2013). “Obtaining natural-like flow releases in diverted river
448 reaches from simple riparian benefit economic models.” Journal of Environmental Management, 118, 161–169.

449 Ramirez-Luna, J. (1997). “Modélisation des ouvrages frontaux et latéraux dans les canaux d’irrigation.” Ph.D. thesis,
450 Ecole Nationale du Génie Rural, des Eaux et des Forêts (ENGREF), Ecole Nationale du Génie Rural, des Eaux et des
451 Forêts (ENGREF), <http://infodoc.agroparistech.fr/index.php?lvl=notice_display&id=125832>.

452 Ramirez-Luna, J., Baume, J., De León-Mojarro, B., Ruiz-Carmona, V., and Sau, J. (1998). “Wave motion stability
453 for coupled canal pool-amil gate systems.” 1998 IEEE International Conference on Systems, Man, and Cybernetics,
454 1998., Vol. 4, IEEE, 3868–3873.

455 Razurel, P., Gorla, L., Crouzy, B., and Perona, P. (2015). “Non-proportional repartition rules optimize environmental
456 flows and energy production.” Water Resources Management, 1–17.

457 Rogers, D. C. and Goussard, J. (1998). “Canal control algorithms currently in use.” Journal of Irrigation and Drainage
458 Engineering, 124(1), 11–15.

459

List of Tables

460

1 Mean values of the dimensionless gate parameters for the four groups and the values used in (Corrigan et al. 1977). 21

461

462

2 Periods and Floquet multipliers for the different periodic solutions shown in Fig. 8 22

TABLE 1. Mean values of the dimensionless gate parameters for the four groups and the values used in (Corrigan et al. 1977).

Group	# of gates	\tilde{Y}_a	\tilde{b}	\tilde{R}	\tilde{r}	ω_F (rad)	θ_c (rad)
1	9	0.448	0.565	0.565	0.665	0.401	0.517
2	8	0.448	0.563	0.633	0.733	0.347	0.440
3	3	0.446	0.560	0.705	0.806	0.264	0.421
4	1	0.450	0.563	0.788	0.888	0.192	0.417
(Corrigan et al. 1977)	1	0.430	0.567	0.633	0.658	0.314	0.434

TABLE 2. Periods and Floquet multipliers for the different periodic solutions shown in Fig. 8

$\frac{c_\omega}{\tilde{c}_{\omega,lim}}$	Free Gate			
	Period	Floquet 1	Floquet 2	Floquet 3
0.999	28.847	1.000	0.996	2.877×10^{-7}
0.998	28.848	1.000	0.992	2.902×10^{-7}
0.996	28.850	1.000	0.985	2.955×10^{-7}
0.990	28.857	1.000	0.962	3.119×10^{-7}
0.980	28.869	1.000	0.923	3.409×10^{-7}
Submerged Gate				
0.999	29.491	1.000	0.996	1.537×10^{-6}
0.998	29.491	1.000	0.992	1.544×10^{-6}
0.996	29.492	1.000	0.984	1.559×10^{-6}
0.990	29.495	1.000	0.961	1.603×10^{-6}
0.980	29.502	1.000	0.922	1.676×10^{-6}

List of Figures

463		
464	1	Photo of an experimental AMIL gate exhibiting oscillating behaviour and creating waves. 24
465	2	Longitudinal and cross-section of gate illustrating the geometric parameters. 25
466	3	Dimensionless gate parameters for 21 typical gate sizes. 26
467	4	Equilibrium position in the projected state space for varying Q'_i . The two components \tilde{d}_A and \tilde{d}_B
468		(above and below gate axis) of the total decrement are shown. 27
469	5	Time evolution (left) and projected state space trajectory (right) of the free gate system as response
470		to a step-like input $Q'_i(\tilde{t})$ for various damping values and level pool lengths (a,b,c). The red, dashed
471		equilibrium curve is superimposed onto the state space plot. Parameters: $\tilde{d}_A = 0.08$; a) $\tilde{c}_\omega = 2.25$,
472		$\tilde{l} = 0.25$; b) $\tilde{c}_\omega = 1.75$, $\tilde{l} = 0.25$; c) $\tilde{c}_\omega = 2.25$, $\tilde{l} = 0.1$; otherwise base parameters from equation (30). 28
473	6	Eigenvalues of the free (top) and submerged (bottom) autonomous gate system for base parameters \mathbf{m}_0
474		and varying \tilde{c}_ω . Left panels: complex plane, right panels: real and imaginary components. 29
475	7	One-parameter bifurcations for the control parameters \tilde{c}_ω , \tilde{l} , and Q'_i , based on the submerged gate with
476		\mathbf{m}_0 . The diagrams show the min./max. value during a limit cycle respectively the equilibrium point in
477		θ_1 and the periods of the limit cycles. Red indicates an unstable, black a stable eq.point/limit cycle.
478		Zoom into the \tilde{c}_ω -values used in Fig. 8 is provided in the supplementary material (Fig. S1). 30
479	8	The time evolution of the gate position and water level during a limit cycle and the trajectory in the
480		state space are shown for the free gate (left) and the submerged gate (right) for various damping ratios.
481		$Q'_i = 0.64$ (free) or $Q'_i = 0.5$ (submerged), otherwise \mathbf{m}_0 31
482	9	Eigenvalues of the submerged gate system for base parameters \mathbf{m}_0 and varying Q'_i 32
483	10	Response in θ_1 and $Q'_g (= Q_g/Q_n)$ of the free (blue, solid) and submerged gate (yellow, dashed) to a
484		step-like increase in Q'_i (green, solid). Besides $Q'_i(\tilde{t})$ (indicated), $\tilde{c}_\omega/\tilde{c}_{\omega,lim} = 0.61$ and \mathbf{m}_0 33
485	11	Limiting damping $\tilde{c}_{\omega,lim}$ as a function of Q'_i for the free gate system (top) with various values for \tilde{d}_A
486		and the submerged gate system (bottom) with $\tilde{d}_{A,0} = 0.02$ and various submergence depths \tilde{Y}_3 34
487	12	Real part of second eigenvalue of linearised systems as a function of level pool length l and for various
488		decrements \tilde{d}_A . The upper plot uses standard damping $\tilde{c}_\omega = \tilde{c}_{\omega,0} = 1.0$ while the lower plot uses a
489		stronger damping of $\tilde{c}_\omega = 1.3$ 35
490	13	Limiting damping $\tilde{c}_{\omega,lim}$ as a function of \tilde{l} for the free (top) and the submerged gate system (bottom)
491		with various values for \tilde{d}_A , otherwise \mathbf{m}_0 36
492	14	Measurements (circles) and model simulations (lines) of the two dynamic behaviours measured on
493		the EPFL gate. The left graph shows three cycles of the oscillating gate, when the standing waves
494		have formed. The right part shows the rising of the gate (blue and orange circles correspond to two
495		measurements of the phenomenon). 37



Fig. 1. Photo of an experimental AMIL gate exhibiting oscillating behaviour and creating waves.

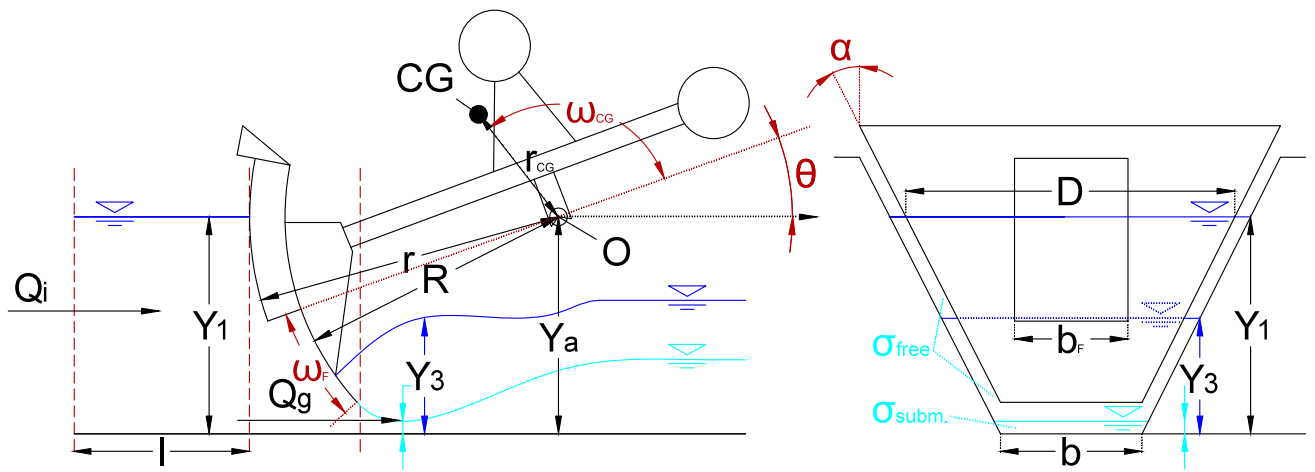


Fig. 2. Longitudinal and cross-section of gate illustrating the geometric parameters.

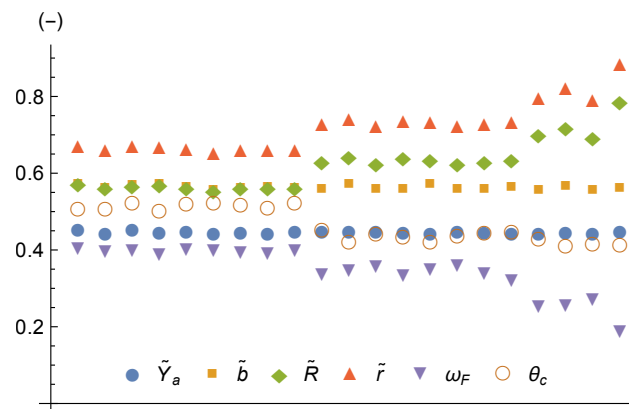


Fig. 3. Dimensionless gate parameters for 21 typical gate sizes.

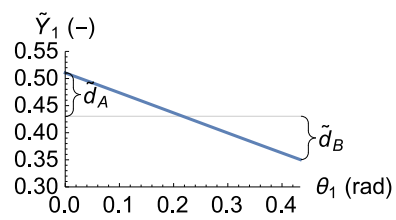


Fig. 4. Equilibrium position in the projected state space for varying Q'_i . The two components \tilde{d}_A and \tilde{d}_B (above and below gate axis) of the total decrement are shown.

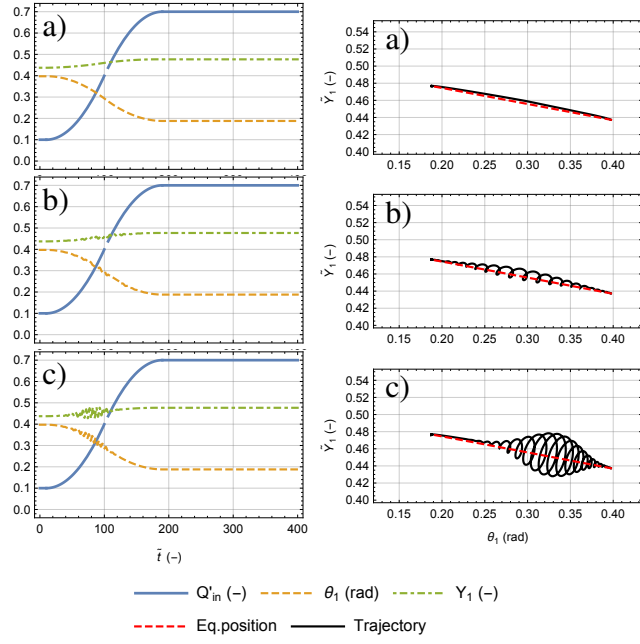


Fig. 5. Time evolution (left) and projected state space trajectory (right) of the free gate system as response to a step-like input $Q'_i(\tilde{t})$ for various damping values and level pool lengths (a,b,c). The red, dashed equilibrium curve is superimposed onto the state space plot. Parameters: $\tilde{d}_A = 0.08$; a) $\tilde{c}_\omega = 2.25$, $\tilde{l} = 0.25$; b) $\tilde{c}_\omega = 1.75$, $\tilde{l} = 0.25$; c) $\tilde{c}_\omega = 2.25$, $\tilde{l} = 0.1$; otherwise base parameters from equation (30).

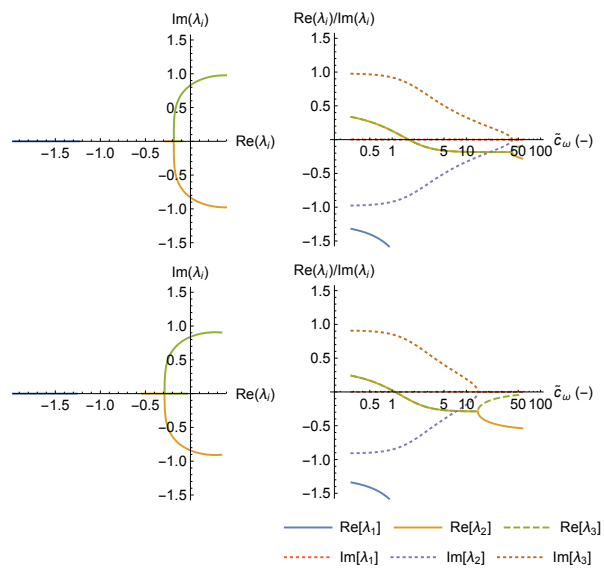


Fig. 6. Eigenvalues of the free (top) and submerged (bottom) autonomous gate system for base parameters \mathbf{m}_0 and varying \tilde{c}_ω . Left panels: complex plane, right panels: real and imaginary components.

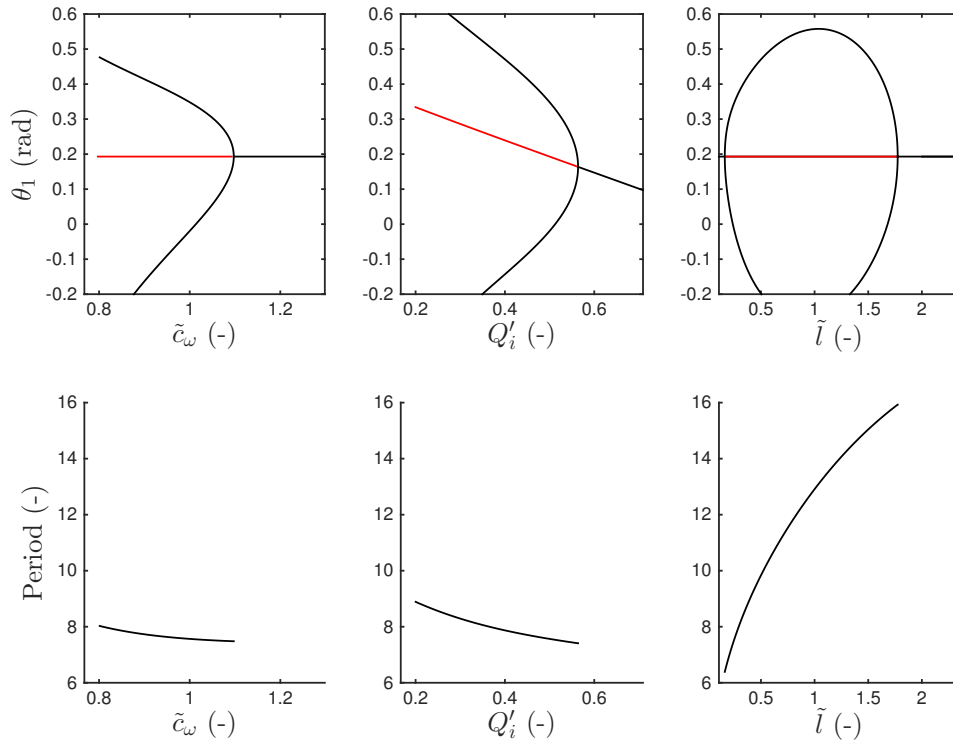


Fig. 7. One-parameter bifurcations for the control parameters \tilde{c}_ω , \tilde{l} , and Q'_i , based on the submerged gate with \mathbf{m}_0 . The diagrams show the min./max. value during a limit cycle respectively the equilibrium point in θ_1 and the periods of the limit cycles. Red indicates an unstable, black a stable eq.point/limit cycle. Zoom into the \tilde{c}_ω -values used in Fig. 8 is provided in the supplementary material (Fig. S1).

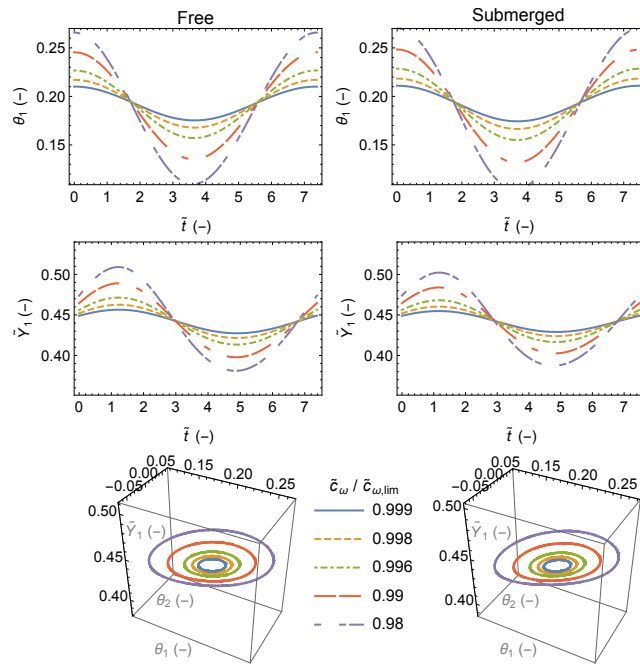


Fig. 8. The time evolution of the gate position and water level during a limit cycle and the trajectory in the state space are shown for the free gate (left) and the submerged gate (right) for various damping ratios. $Q'_i = 0.64$ (free) or $Q'_i = 0.5$ (submerged), otherwise \mathbf{m}_0 .

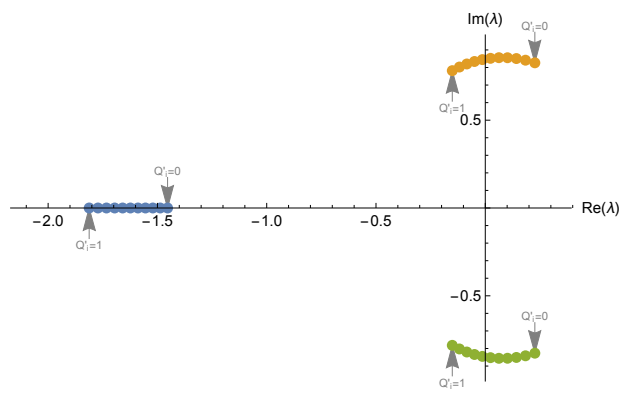


Fig. 9. Eigenvalues of the submerged gate system for base parameters \mathbf{m}_0 and varying Q'_i .

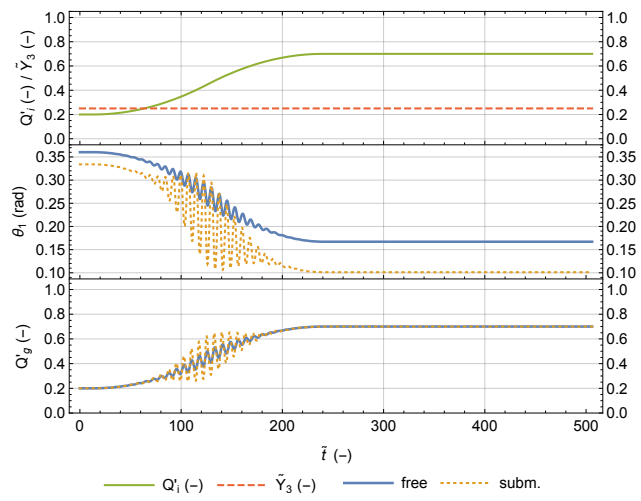


Fig. 10. Response in θ_1 and Q'_g ($= Q_g/Q_n$) of the free (blue, solid) and submerged gate (yellow, dashed) to a step-like increase in Q'_i (green, solid). Besides $Q'_i(\tilde{t})$ (indicated), $\tilde{c}_\omega/\tilde{c}_{\omega,lim} = 0.61$ and \mathbf{m}_0 .

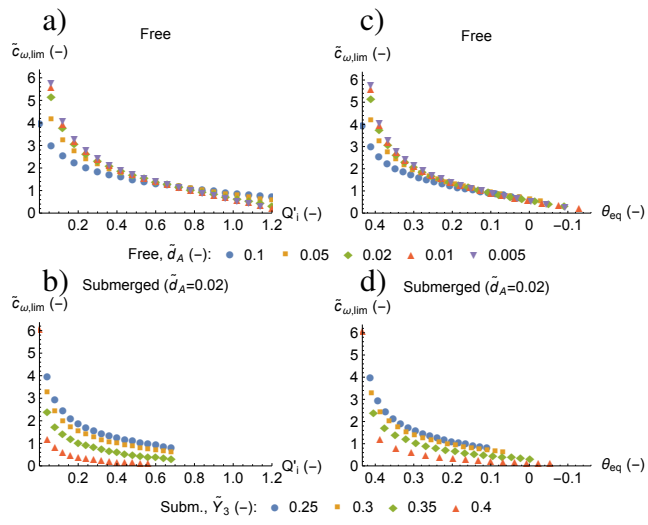


Fig. 11. Limiting damping $\tilde{c}_{\omega,lim}$ as a function of Q'_i for the free gate system (top) with various values for \tilde{d}_A and the submerged gate system (bottom) with $\tilde{d}_{A,0} = 0.02$ and various submergence depths \tilde{Y}_3 .

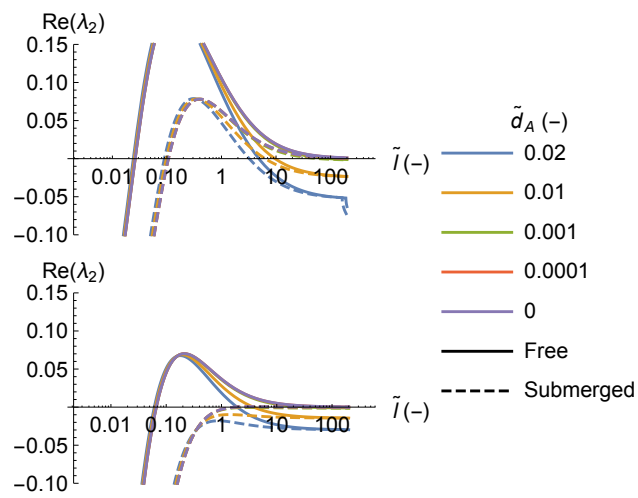


Fig. 12. Real part of second eigenvalue of linearised systems as a function of level pool length l and for various decrements \tilde{d}_A . The upper plot uses standard damping $\tilde{c}_\omega = \tilde{c}_{\omega,0} = 1.0$ while the lower plot uses a stronger damping of $\tilde{c}_\omega = 1.3$.

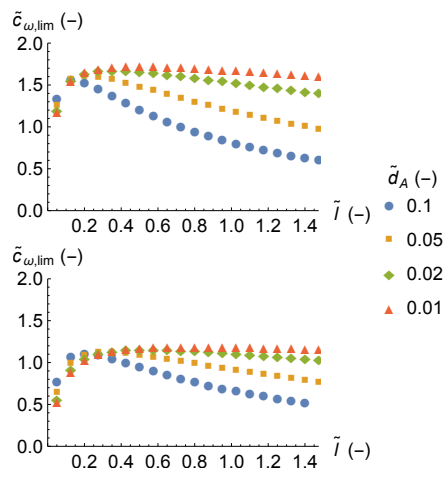


Fig. 13. Limiting damping $\tilde{c}_{\omega,lim}$ as a function of \tilde{l} for the free (top) and the submerged gate system (bottom) with various values for \tilde{d}_A , otherwise \mathbf{m}_0 .

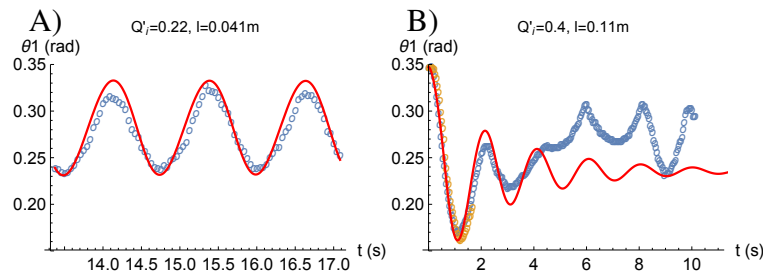



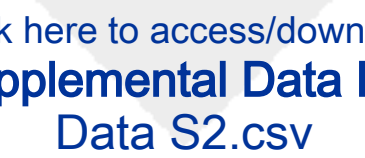
Fig. 14. Measurements (circles) and model simulations (lines) of the two dynamic behaviours measured on the EPFL gate. The left graph shows three cycles of the oscillating gate, when the standing waves have formed. The right part shows the rising of the gate (blue and orange circles correspond to two measurements of the phenomenon).







Click here to access/download
Supplemental Data File
Captions_ESM.txt





Click here to access/download
Supplemental Data File
Data S2.csv



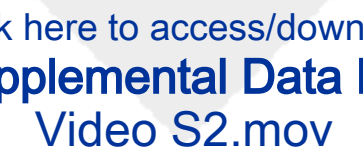


Click here to access/download
Supplemental Data File
Data S3.csv



Click here to access/download
Supplemental Data File
Figure S1.pdf





Click here to access/download
Supplemental Data File
Video S2.mov





Click here to access/download
Supplemental Data File
Video S3.mov



ASCE Authorship, Originality, and Copyright Transfer Agreement

Publication Title: Journal of Irrigation and Drainage Engineering

Manuscript Title: Dynamical Behaviour and Stability Analysis of Hydraulomechanical Gates

Author(s) – Names, postal addresses, and e-mail addresses of all authors

Fabian Alexander Bernhard, EPFL ENAC CRYOS, GRAO 392, Station 2,
CH-1015 Lausanne, SWITZERLAND ; fabian.bernhard@alumni.epfl.ch

Paolo Perona, William Rankine Building, The University of Edinburgh, The King's Buildings,
Mayfield Road, Edinburgh EH9 3JL, UK ; paolo.perona@ed.ac.uk

I. Authorship Responsibility

To protect the integrity of authorship, only people who have significantly contributed to the research or project and manuscript preparation shall be listed as coauthors. The corresponding author attests to the fact that anyone named as a coauthor has seen the final version of the manuscript and has agreed to its submission for publication. Deceased persons who meet the criteria for coauthorship shall be included, with a footnote reporting date of death. No fictitious name shall be given as an author or coauthor. An author who submits a manuscript for publication accepts responsibility for having properly included all, and only, qualified coauthors.

I, the corresponding author, confirm that the authors listed on the manuscript are aware of their authorship status and qualify to be authors on the manuscript according to the guidelines above.

Fabian Bernhard
Print Name


Signature

28 February 2017
Date

II. Originality of Content

ASCE respects the copyright ownership of other publishers. ASCE requires authors to obtain permission from the copyright holder to reproduce any material that (1) they did not create themselves and/or (2) has been previously published, to include the authors' own work for which copyright was transferred to an entity other than ASCE. Each author has a responsibility to identify materials that require permission by including a citation in the figure or table caption or in extracted text. Materials re-used from an open access repository or in the public domain must still include a citation and URL, if applicable. At the time of submission, authors must provide verification that the copyright owner will permit re-use by a commercial publisher in print and electronic forms with worldwide distribution. For Conference Proceeding manuscripts submitted through the ASCE online submission system, authors are asked to verify that they have permission to re-use content where applicable. Written permissions are not required at submission but must be provided to ASCE if requested. Regardless of acceptance, no manuscript or part of a manuscript will be published by ASCE without proper verification of all necessary permissions to re-use. ASCE accepts no responsibility for verifying permissions provided by the author. Any breach of copyright will result in retraction of the published manuscript.

I, the corresponding author, confirm that all of the content, figures (drawings, charts, photographs, etc.), and tables in the submitted work are either original work created by the authors listed on the manuscript or work for which permission to re-use has been obtained from the creator. For any figures, tables, or text blocks exceeding 100 words from a journal article or 500 words from a book, written permission from the copyright holder has been obtained and supplied with the submission.

Fabian Bernhard
Print name


Signature

28 February 2017
Date

III. Copyright Transfer

ASCE requires that authors or their agents assign copyright to ASCE for all original content published by ASCE. The author(s) warrant(s) that the above-cited manuscript is the original work of the author(s) and has never been published in its present form.

The undersigned, with the consent of all authors, hereby transfers, to the extent that there is copyright to be transferred, the exclusive copyright interest in the above-cited manuscript (subsequently called the "work") in this and all subsequent editions of the work (to include closures and errata), and in derivatives, translations, or ancillaries, in English and in foreign translations, in all formats and media of expression now known or later developed, including electronic, to the American Society of Civil Engineers subject to the following:

- The undersigned author and all coauthors retain the right to revise, adapt, prepare derivative works, present orally, or distribute the work, provided that all such use is for the personal noncommercial benefit of the author(s) and is consistent with any prior contractual agreement between the undersigned and/or coauthors and their employer(s).
- No proprietary right other than copyright is claimed by ASCE.
- If the manuscript is not accepted for publication by ASCE or is withdrawn by the author prior to publication (online or in print), this transfer will be null and void.
- Authors may post a PDF of the ASCE-published version of their work on their employers' **Intranet** with password protection. The following statement must appear with the work: "This material may be downloaded for personal use only. Any other use requires prior permission of the American Society of Civil Engineers."
- Authors may post the **final draft** of their work on open, unrestricted Internet sites or deposit it in an institutional repository when the draft contains a link to the published version at www.ascelibrary.org. "Final draft" means the version submitted to ASCE after peer review and prior to copyediting or other ASCE production activities; it does not include the copyedited version, the page proof, a PDF, or full-text HTML of the published version.

Exceptions to the Copyright Transfer policy exist in the following circumstances. Check the appropriate box below to indicate whether you are claiming an exception:

U.S. GOVERNMENT EMPLOYEES: Work prepared by U.S. Government employees in their official capacities is not subject to copyright in the United States. Such authors must place their work in the public domain, meaning that it can be freely copied, republished, or redistributed. In order for the work to be placed in the public domain, ALL AUTHORS must be official U.S. Government employees. If at least one author is not a U.S. Government employee, copyright must be transferred to ASCE by that author.

CROWN GOVERNMENT COPYRIGHT: Whereby a work is prepared by officers of the Crown Government in their official capacities, the Crown Government reserves its own copyright under national law. If ALL AUTHORS on the manuscript are Crown Government employees, copyright cannot be transferred to ASCE; however, ASCE is given the following nonexclusive rights: (1) to use, print, and/or publish in any language and any format, print and electronic, the above-mentioned work or any part thereof, provided that the name of the author and the Crown Government affiliation is clearly indicated; (2) to grant the same rights to others to print or publish the work; and (3) to collect royalty fees. ALL AUTHORS must be official Crown Government employees in order to claim this exemption in its entirety. If at least one author is not a Crown Government employee, copyright must be transferred to ASCE by that author.

WORK-FOR-HIRE: Privately employed authors who have prepared works in their official capacity as employees must also transfer copyright to ASCE; however, their employer retains the rights to revise, adapt, prepare derivative works, publish, reprint, reproduce, and distribute the work provided that such use is for the promotion of its business enterprise and does not imply the endorsement of ASCE. In this instance, an authorized agent from the authors' employer must sign the form below.

U.S. GOVERNMENT CONTRACTORS: Work prepared by authors under a contract for the U.S. Government (e.g., U.S. Government labs) may or may not be subject to copyright transfer. Authors must refer to their contractor agreement. For works that qualify as U.S. Government works by a contractor, ASCE acknowledges that the U.S. Government retains a nonexclusive, paid-up, irrevocable, worldwide license to publish or reproduce this work for U.S. Government purposes only. This policy DOES NOT apply to work created with U.S. Government grants.

I, the corresponding author, acting with consent of all authors listed on the manuscript, hereby transfer copyright or claim exemption to transfer copyright of the work as indicated above to the American Society of Civil Engineers.

Fabian Bernhard

Print Name of Author or Agent



Signature of Author or Agent

28 February 2017

Date

More information regarding the policies of ASCE can be found at <http://www.asce.org/authorsandeditors>



No comments needed to be addressed.